Search for light gauge bosons of the dark sector at MAMI

H. Merkel,[1, *] P. Achenbach,[1] C. Ayerbe Gayoso,[1] J. C. Bernauer,[1, †] R. Böhm,[1] D. Bosnar,[2] L. Debenjak,[3]
A. Denig,[1] M. O. Distler,[1] A. Esser,[1] H. Fonvieille,[4] I. Friščić,[2] D. G. Middleton,[1] U. Müller,[1] L. Nungesser,[1]
J. Pochodzalla,[1] M. Rohrbeck,[1] S. Sánchez Majos,[1] B. S. Schlimme,[1] M. Schoth,[1] S. Širca,[3, 5] and M. Weinriefer[1]
(A1 Collaboration)
[1]*Institut für Kernphysik, Johannes Gutenberg-Universität Mainz, D-55099 Mainz, Germany.*[‡]
[2]*Department of Physics, University of Zagreb, HR-10002 Zagreb, Croatia.*
[3]*Jožef Stefan Institute, SI-1000 Ljubljana, Slovenia.*
[4]*Clermont Université, Université Blaise Pascal, CNRS/IN2P3, LPC, BP 10448, F-63000 Clermont-Ferrand, France.*
[5]*Department of Physics, University of Ljubljana, SI-1000 Ljubljana, Slovenia.*

(Dated: January 21, 2011)

A new exclusion limit for the electromagnetic production of a light $U(1)$ gauge boson γ' decaying to e^+e^- was determined by the A1 Collaboration at the Mainz Microtron MAMI. Such light gauge bosons appear in several extensions of the standard model and are also discussed as candidates for the interaction of dark matter with Standard Model matter. In electron scattering from a heavy nucleus, the existing limits for a narrow state coupling to e^+e^- were reduced by nearly an order of magnitude in the range of the lepton pair mass of $210\,\mathrm{MeV}/c^2 < m_{e^+e^-} < 300\,\mathrm{MeV}/c^2$. This experiment demonstrates the potential of high current and high resolution fixed target experiments for the search for physics beyond the Standard Model.

PACS numbers: 95.30.Cq, 14.70.Pw, 25.30.Rw

INTRODUCTION

An additional $U(1)$ interaction appears natural in nearly all theoretical extensions of the Standard Model. Large gauge symmetries have to be broken and $U(1)$ bosons provide the lowest-rank local symmetries. *E.g.* in standard embedding of most variants of string theories a $U(1)$ boson is generated by symmetry breaking. Such additional $U(1)$ bosons may be hidden, *e.g.* no Standard Model particles are charged under them, but their mass is allowed in the range of the Standard Model masses.

Recently, several experimental anomalies were discussed as possible signature for a hidden force. A light $U(1)$ boson in the mass range below $1\,\mathrm{GeV}/c^2$ might explain *e.g.* the observed anomaly of the muon magnetic moment [1]. Cosmology and astrophysics provide an abundant amount of evidence for the existence of dark matter (for a summary see *e.g.* Ref. [2]). Several experimental hints point to a $U(1)$ boson coupling to leptons as the mediator of the interaction of dark matter with Standard Model matter (see *e.g.* Ref. [3] for a detailed discussion). For example the lively debated annual modulation signal of the DAMA/LIBRA experiment [4] could be brought into accordance with the null result of bolometric experiments if one assumes an interaction via a light $U(1)$ boson [3]. Observations of cosmic rays show a positron excess [5]. While this excess may be due to astrophysical process like quasars, this could also be a hint for the annihilation of dark matter into leptons. If the experimental evidence is interpreted as annihilation of dark matter, the excess of positrons and no excess of anti-protons in cosmic rays hints again to a mass of the $U(1)$ boson below $2\,\mathrm{GeV}/c^2$.

The interaction strength of such a $U(1)$ boson (in the following denoted as γ', in the literature also denoted as A', U, or ϕ) is governed by the mechanism of kinetic mixing [6]. The coupling can be subsumed by an effective coupling constant ϵ and a vertex structure of a massive photon.

Bjorken *et al.* [7] discussed several possible experimental schemes for the search of a γ' in the most likely mass range of a few MeV/c^2 up to a few GeV/c^2. Since the coupling is small, the cross-section for electro-magnetic production of the γ' boson can be enhanced by a factor Z^2 by choosing a heavy nucleus as the target (see Fig. 1). The subsequent decay of the γ' boson to a lepton pair is the signature of the reaction.

The cross section of signal and background were estimated in Ref. [7] in the Weizsäcker-Williams-approximation. In this approximation, the cross section shows a sharp peak, both in signal and background, where nearly all the energy of the incident electron is transferred to the lepton pair $(E_{e^+} + E_{e^-}) = E_0$. Correspondingly, the pair is produced dominantly in the direction of the incident electron.

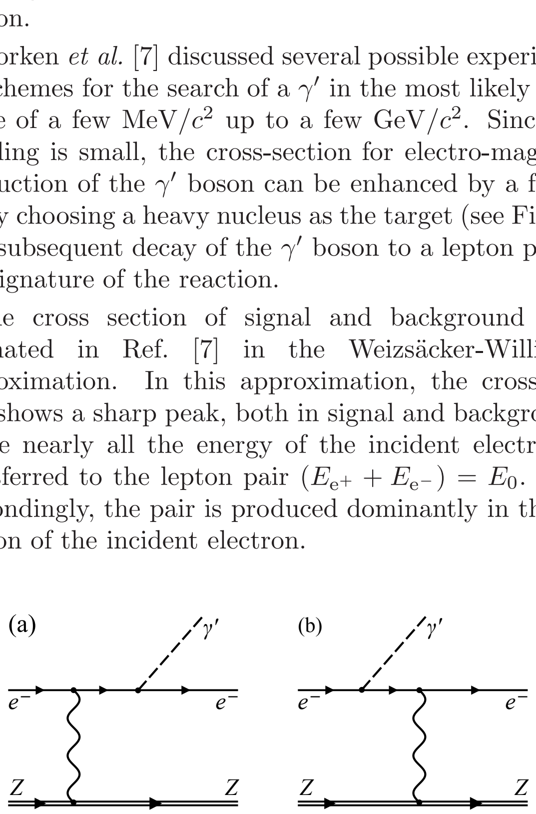

FIG. 1. Electromagnetic production of the γ' boson. The coupling of the γ' boson is parametrized as $i\,\epsilon\, e\, \gamma^\mu$.

The experimental challenge is the suppression of the background which is dominated by radiative pair production (Fig. 2). Radiation by the final or initial electron (graph (a) and (b) of Fig. 2) has the same cross section structure as the desired signal and is an irreducible background to this experiment. Radiation with an internal lepton line (graph (c) and (d) of Fig. 2) has a maximum if the internal electron line is nearly on mass shell, *i.e.* if one of the leptons carries nearly all the energy of the pair. This background can be reduced by choosing a kinematic setting in which the electron and positron are detected at equal angles and momenta.

EXPERIMENT

The experiment took place at the spectrometer setup of the A1 collaboration at MAMI (see Ref. [8] for a detailed description). An unpolarized electron beam with a beam energy of $E_0 = 855\,\mathrm{MeV}$ and a beam current of $90\,\mu\mathrm{A}$ was incident on a Tantalum foil (99.9% $^{181}\mathrm{Ta}$, $Z = 73$) with an area density of $81.3\,\mathrm{mg/cm^2}$, leading to a luminosity of $L\,Z^2 = 8.07 \cdot 10^{38}\,\mathrm{s^{-1}cm^{-2}}$. The beam was rastered across the target to reduce the local thermal load on the target foil.

For the detection of the electron-positron pair two high resolution spectrometers were used. The particles were detected by vertical drift chambers for tracking and scintillator detectors for trigger and timing purpose. In addition, a threshold-gas-Čerenkov detector was used in each arm to discriminate between electrons/positrons and pions.

Table I summarizes the kinematic set-ups used. Setup 1 was chosen to be close to $E_{e^+} + E_{e^-} = E_0$ where the cross section has a sharp peak to ensure high count rates. In addition, set-up 2 was selected at $E_{e^+} + E_{e^-} = 0.9\,E_0$ during the experiment to optimize the total count rates. The angles of the spectrometers were set to be nearly symmetric to reduce the background by the Bethe-Heitler-process (Fig. 2, graphs (c) and (d)). In total, data of four days of beam time were used for the analysis. The electrons and the positrons were detected by the coincidence of the raw scintillator signals. The Čerenkov signals were not included in the trigger logic but recorded for offline analysis.

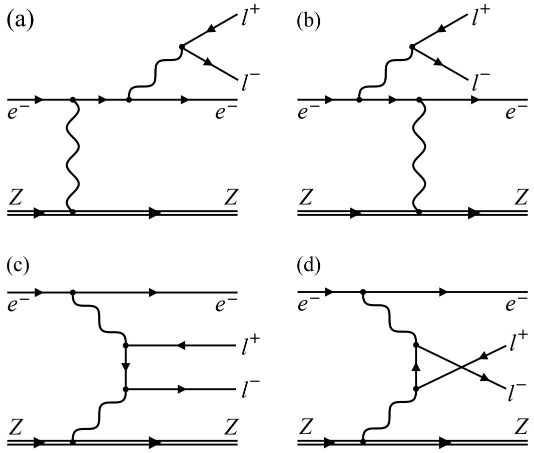

FIG. 2. Dominant background processes. While graphs (a) and (b) have the same structure as the signal and present an irreducible background, the contributions of graphs (c) and (d) can be suppressed by the choice of kinematic setting.

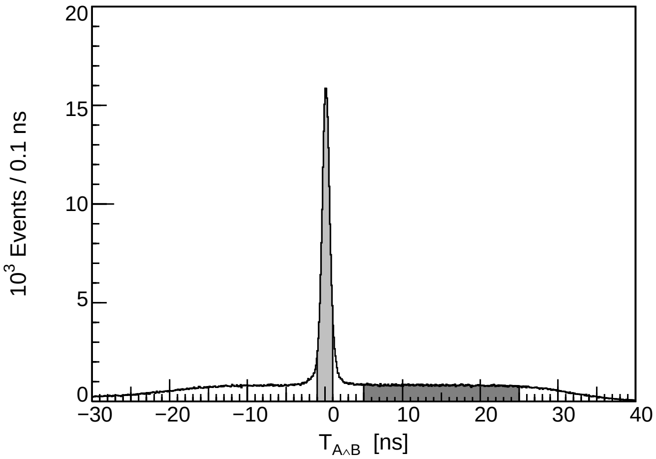

FIG. 3. Coincidence time distribution after particle identification by Čerenkov detectors. The events of the light shaded area were used as true coincidences, while the dark shaded area was used as estimate of the accidental coincidences.

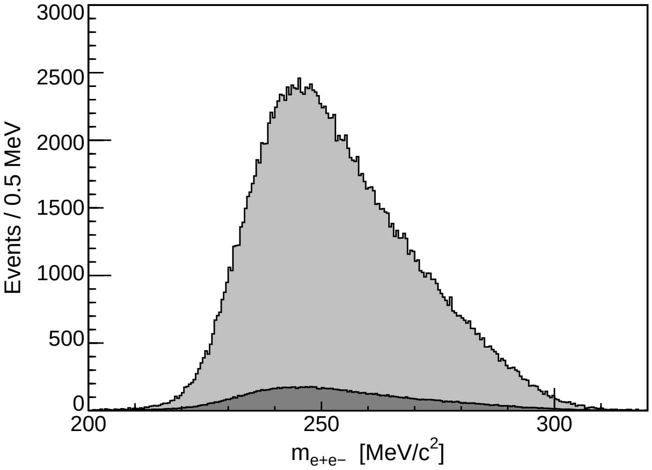

FIG. 4. Mass distribution of the reconstructed e^+-e^--pair. The dark shaded area denotes the background due to accidental coincidences (scaled to a time window of 2 ns).

DATA ANALYSIS

Only events with a positive signal in the Čerenkov detectors were selected with an efficiency of 98% for

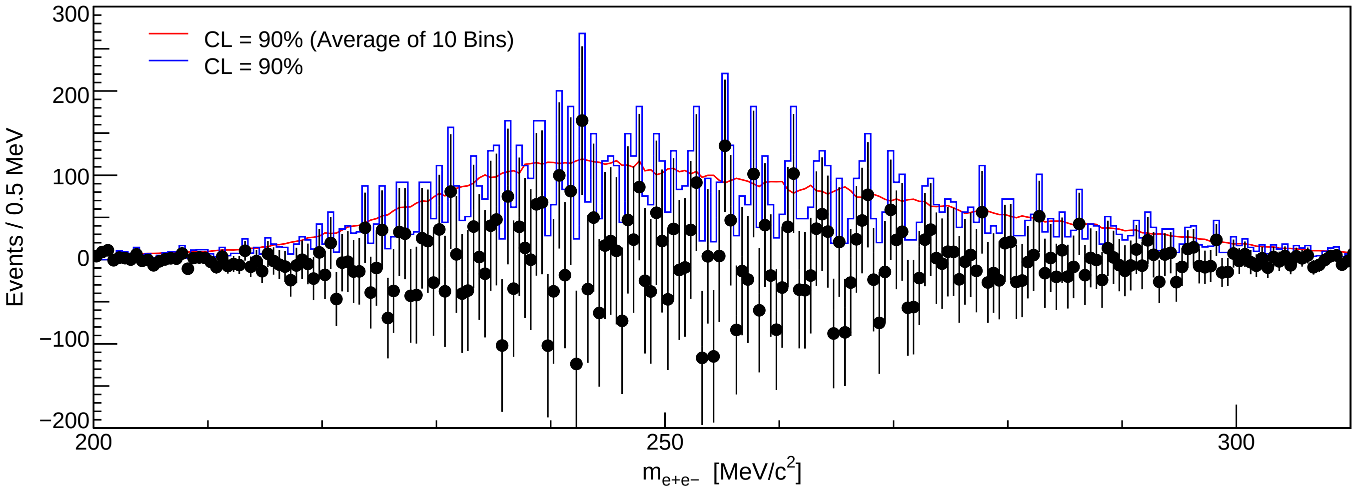

FIG. 5. Upper exclusion limits with 90% confidence level determined by the Feldman-Cousins algorithm (color online). The averaged limit is included for subjective judgement only (≈ 10% of the data points should be above this line at 90% CL).

	Spectrometer A (e^+)			Spectrometer B (e^-)		
	p (MeV)	θ	$d\Omega$ (msr)	p (MeV)	θ	$d\Omega$ (msr)
Set-up 1	346.3	22.8°	21	507.9	15.2°	5.6
Set-up 2	338.0	22.8°	21	469.9	15.2°	5.6

TABLE I. Kinematic settings. The incident beam energy was $E_0 = 855\,\mathrm{MeV}$, the settings are roughly centered around $E_{e^+} + E_{e^-} = E_0$ and $m_{\gamma'} = 250\,\mathrm{MeV}/c^2$.

spectrometer A and 95% for spectrometer B [8]. Figure 3 shows the coincidence time between the corresponding spectrometers after correction for the flight path of ≈ 12 m within the spectrometers for these events. A timing resolution of better than 1 ns FWHM was achieved, a cut of $-1\,\mathrm{ns} < t_{\mathrm{A}\wedge\mathrm{B}} < 1\,\mathrm{ns}$ was used to mark the true electron/positron pairs. Below the peak a background due to accidental coincidences is present. To correct for this background, events in the coincidence side band $5\,\mathrm{ns} < t_{\mathrm{A}\wedge\mathrm{B}} < 25\,\mathrm{ns}$ were selected and weighted by the ratio of the timing windows.

For the real electron/positron pairs the invariant mass squared of the pair was determined by the four momentum sum $m^2_{e^+e^-} = (p_{e^+} + p_{e^-})^2$. Figure 4 shows the resulting mass spectrum. The contribution of accidental background is indicated by the dark shaded area.

In this figure, a possible candidate for the dark photon would appear as a peak on top of the background. The width of such a peak can only be estimated by simulation. For this, the experimental resolution of the four vector determination of a single spectrometer was determined by the width of the lowest lines of the nuclear excitation spectrum in elastic electron scattering. This single spectrometer resolution was used as input for the simulation of the experiment. A mass resolution of better than $0.5\,\mathrm{MeV}/c^2$ was determined, corresponding to the chosen bin width in Fig. 4.

No significant peak in the mass spectrum was observed. The corresponding upper limit was determined by the Feldman-Cousins algorithm [9]. As input for this algorithm the raw mass spectrum was used and as a background estimate for each bin the mean of the three neighboring bins on either side was used. This choice of the background estimate introduces systematic errors, which have to be investigated in the case of a positive signal, but only enhance statistical fluctuations in the case of an upper limit. Figure 5 shows the resulting exclusion limits.

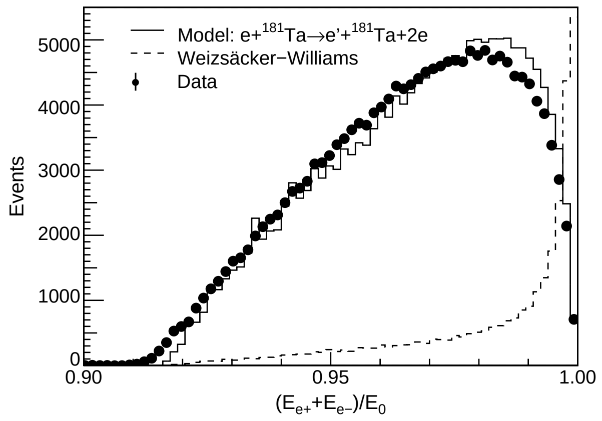

FIG. 6. Comparison of simulation with data. As model the coherent electro-production from a heavy nucleus was used.

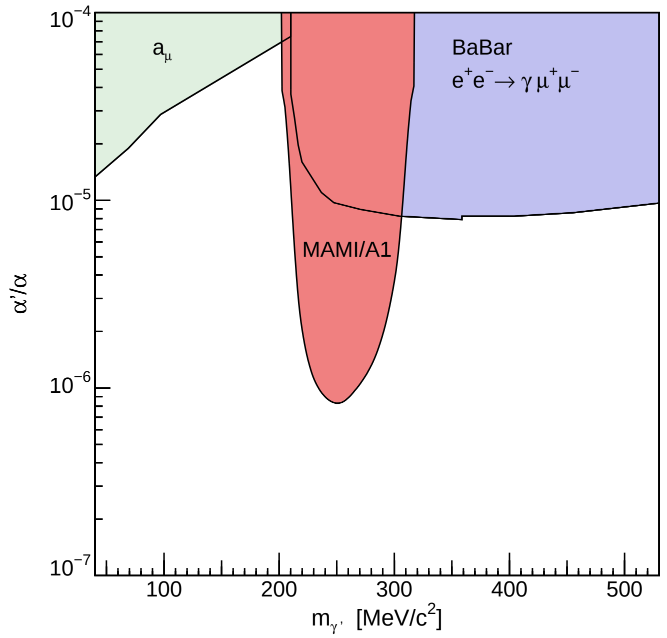

FIG. 7. Exclusion limits with 90% confidence level in terms of relative coupling $\alpha'/\alpha = \epsilon^2$ (color online). Also shown are the previous results by BaBar [10] and for a_μ of the muon [1].

RESULTS AND INTERPRETATION

In order to interpret the result in terms of the effective coupling ϵ of a possible dark photon candidate, a model for the production process has to be used. Unfortunately, it turns out that the Weizsäcker-Williams-approximation used in Ref. [7] fails in this energy range by orders of magnitude, mainly since the recoil of the nucleus cannot be neglected. Taking into account the nuclear recoil, the peak at $(E_{e^+}+E_{e^-}) = E_0$ in Ref. [7] is regularized and the cross section at this point becomes zero. In addition, the assumption of a real initial photon exactly in direction of the electron beam introduces a peak in the angular distribution, which is not present in electro-production due to helicity conservation of the scattered electron.

Instead, we used as a model for the γ' production the coherent electro-production from the Tantalum nucleus, calculated as the coherent sum of the graphs of Fig. 1. The charge distribution of Tantalum was approximated as a solid sphere. For the QED background we used the coherent sum of the graphs of Fig. 2. The corresponding cross sections were included on an event by event basis in the simulation. The simulation including this model shows excellent agreement with data, as demonstrated in Fig. 6, where the background subtracted yields as an estimate for the QED background graphs is compared to the simulation of this process.

The remaining model dependence of this interpretation mainly affects the nuclear vertex, since *e.g.* the possible breakup of the recoil nucleus is neglected. Since this vertex is common to both the signal and the QED background channels, to further reduce the model dependence we use only the ratio of signal to QED background of the simulation in addition to the accidental background. The ratio can be translated to the effective coupling for a given mass resolution δ_m by using Eqn. (19) of Ref. [7]

$$\frac{d\sigma(\mathrm{X} \rightarrow \gamma'\,\mathrm{Y} \rightarrow \mathrm{e}^+\mathrm{e}^-\mathrm{Y})}{d\sigma(\mathrm{X} \rightarrow \gamma^*\mathrm{Y} \rightarrow \mathrm{e}^+\mathrm{e}^-\mathrm{Y})} = \frac{3\pi}{2N_\mathrm{f}}\,\frac{\epsilon^2}{\alpha}\,\frac{m_{\gamma'}}{\delta_m}$$

and the measured event rate as estimate for the background channel. The number of final states N_f includes the ratio of phase space for the corresponding decays above the $\mu^+\mu^-$ threshold.

Figure 7 shows the result of this experiment in terms of the ratio of the effective coupling to the fine structure constant $\alpha'/\alpha = \epsilon^2$. For clarity of the figure, the exclusion limit was averaged. Also shown are the existing limits published by BaBar [10] and the Standard Model prediction [1] of the muon anomalous magnetic moment $a_\mu = g_\mu/2 - 1$. The existing exclusion limit has been extended by an order of magnitude.

In this experiment, the discovery potential of the existing high luminosity electron accelerators has been demonstrated. The background conditions are well under control due to excellent timing and missing mass resolution. An extensive program to cover further mass regions with similar experiments is planned at MAMI and Jefferson Lab [11].

The authors would like to thank the MAMI accelerator group for providing the excellent beam quality and intensity necessary for this experiment, and T. Beranek for fruitful discussions on the QED calculations. This work was supported by the Federal State of Rhineland-Palatinate and by the Deutsche Forschungsgemeinschaft with the Collaborative Research Center 443.

---

[*] merkel@kph.uni-mainz.de
[†] Now at MIT-LNS, Cambridge, MA, U.S.A.
[‡] http://www.kph.uni-mainz.de

[1] M. Pospelov, Phys. Rev., **D80**, 095002 (2009).

[2] K. Nakamura *et al.* (Particle Data Group), J. Phys., **G37**, 075021 (2010).

[3] N. Arkani-Hamed, D. P. Finkbeiner, T. R. Slatyer, and N. Weiner, Phys. Rev., **D79**, 015014 (2009).

[4] R. Bernabei *et al.*, Eur. Phys. J., **C56**, 333 (2008).

[5] O. Adriani *et al.*, Nature, **458**, 607 (2009).

[6] B. Holdom, Phys. Lett., **B166**, 196 (1986).

[7] J. D. Bjorken, R. Essig, P. Schuster, and N. Toro, Phys. Rev., **D80**, 075018 (2009).

[8] K. I. Blomqvist *et al.*, Nucl. Instrum. Meth., **A403**, 263 (1998).

[9] G. J. Feldman and R. D. Cousins, Phys. Rev., **D57**, 3873 (1998).

[10] B. Aubert *et al.*, Phys. Rev. Lett., **103**, 081803 (2009).

[11] R. Essig, P. Schuster, N. Toro, and B. Wojtsekhowski, (2010), arXiv:1001.2557 [hep-ph].